

Musical Instrument Separation on Shift-Invariant Spectrograms via Stochastic Dictionary Learning

Sören Schulze^{1,*} and Emily J. King¹

¹*AG Computational Data Analysis, Faculty 3, University of Bremen*

**Corresponding author: sschulze@math.uni-bremen.de*

July 14, 2022

We propose a method for the blind separation of audio signals from musical instruments. While the approach of applying non-negative matrix factorization (NMF) has been studied in many papers, it does not make use of the pitch-invariance that instruments exhibit. This limitation can be overcome by using tensor factorization, in which context the use of log-frequency spectrograms was initiated, but this still requires the specific tuning of the instruments to be hard-coded into the algorithm. We develop a time-frequency representation that is both shift-invariant and frequency-aligned, with a variant that can also be used for wideband signals. Our separation algorithm exploits this shift-invariance in order to find patterns of peaks related to specific instruments, while non-linear optimization enables it to represent arbitrary frequencies and incorporate inharmonicity, and the reasonability of the representation is ensured by a sparsity condition. The relative amplitudes of the harmonics are saved in a dictionary, which is trained via a modified version of ADAM. For a realistic monaural piece with acoustic recorder and violin, we achieve qualitatively good separation with a signal-to-distortion ratio (SDR) of 12.7 dB, a signal-to-interference ratio (SIR) of 27.0 dB, and a signal-to-artifacts ratio (SAR) of 12.9 dB, averaged.

1 Introduction

1.1 Related Work and Approach

Dictionary learning is a very popular technique for the blind separation of audio sources, both of music recordings as well as of speech signals. Classically, this is done via application of the short-time Fourier transform (STFT) [cf. 15] on the audio signal and decomposition of the resulting spectrogram (i.e., the magnitude of the STFT) via non-negative matrix factorization (NMF) [21]. This approach was initially studied by Smaragdis and Brown

[26] for the purpose of polyphonic music transcription and then applied to audio source separation by Wang and Plumbley [29].

In many cases, a single musical instrument can generate different sounds which are perceptually similar but only vary in the pitch of the tones. In the STFT spectrogram, different pitch manifests in linear scaling of the distances between the peaks in the frequency axis, which is computationally hard to handle. Therefore, Fitzgerald et al. [11] applied the constant-Q transform (CQT) [8], which turns scaling into shifts, and developed the shifted non-negative matrix factorization (SNMF) in order to train a shift-invariant dictionary. This approach was later refined by Jaiswal et al. [16, 17, 18].

While the constant-Q transform ensures the shift-invariance of patterns of sinusoids when varying the pitch, its transient response varies with frequency. To overcome this, the scattering transform by Andén and Mallat [3] subsequently employs smoothing in the time domain.

Another approach is the computation of the Mel spectrogram [25], which applies logarithmically spaced windows in the frequency direction. This, however, unfavorably attenuates sinusoids compared to transients in the higher frequencies.

The Heisenberg inequality [cf. 15, 13] sets a fundamental bound to the time-frequency resolution achievable. If we use Gaussian windows where ζ is the standard deviation of the window in the time domain and σ is the standard deviation of its Fourier transform, then we have $\zeta \cdot \sigma \geq 1/(2\pi)$. If, for instance, $\zeta = 20$ ms, then $\sigma \approx 7.96$ Hz. For speech processing, this may be sufficient, but considering music that contains frequencies as low as 20 Hz, this deviation equals almost half an octave (or a tritone).

Whereas this low resolution may be acceptable for low frequencies where tight intervals are rare, conveying it to higher frequencies for the sake of shift-invariance is infeasible. Instead, we rely on sparsity-based techniques and prior information about the images of the tones in the spectrogram in order to sharpen the lines beyond the limit determined by the Heisenberg inequality.

1.2 The Musical Role of Sparsity

The difficulty of blind separation can be illustrated with the pipe organ instrument [cf. 12, 5], which is commonly found in churches, concert halls, and some theaters. Simply speaking, a pipe organ has a number of organ stops which can be played alone as individual instruments but are typically combined such they sound together when a key is pressed.

Some organ stops are designed to have a fundamental frequency that is different from that of the tone to be played, and instead fits in its harmonic series, such that the combination of the organs stops creates an artificial harmonic pattern and thereby the illusion of a single musical instrument.

Without any prior information, there are several valid approaches how to save the sound of a pipe organ in a dictionary. It is possible to treat each organ stop as an individual instrument and represent the combined sound as a linear combination of all the organ stops involved. If one organ stop is just a pitch-shifted version of another, those two may even share a dictionary entry.

While this approach seems sensible, the algorithm has no universal way to distinguish between a harmonic-rich organ stop and a combination of harmonic-poor organ stops. In the extreme case, it is possible to construct the spectrum by the unrealistic assumption of a

single instrument with a sinusoidal sound, which plays a large number of tones at the same time.

To discourage this solution, it is essential to limit the number of simultaneous tones. Mathematically speaking, this is a sparsity condition; it makes those representations more favorable to the algorithm which treat combinations of organ stops as individual instruments. On the other hand, the number of possible combinations of organ stops is exponential, so such representations may require a large dictionary size. If the number of possible instruments is chosen too large, however, then the algorithm may assign polyphonic sounds (with multiple keys pressed) to single instruments for stricter sparsity; in the extreme case, each time frame could have its own instruments, with no relation to the others.

In the end, there is no universal notion of an “instrument” just from the audio recording. While there are cases in which the distinction of instruments may be more obvious to human listeners than for the pipe organ, it is always a challenge to convey these expectations to the algorithm. Both the size of the dictionary and the sparsity constraint for the representation must be chosen very carefully in order to yield an intuitively meaningful solution. Separation works best if the number of instruments to separate is known, the instruments can be clearly distinguished via their harmonic spectra, and polyphony is limited.

2 Computation of the Spectrogram

2.1 Narrowband Signals

The dictionary learning algorithm is supposed to operate on a spectrogram, which is a non-negative time-frequency representation of the audio recording. We require the spectrogram to be shift-invariant, such that multiplying the frequency of a sinusoidal signal by a fixed factor causes a fixed shift of its image in the spectrogram. At the same time, the image of a δ -transient should be uniform along the frequency axis.

The first requirement is fulfilled by the CQT introduced by Brown [8]; this method was later generalized by Balazs et al. [4]. In the scattering transform [3], the CQT is interpreted as a Morlet wavelet transform; afterwards, the modulus is convolved with a smoothing kernel in order to widen the transient response in the higher frequencies.

We take this concept a step further by designing the kernel such that the transient response is frequency-uniform. First of all, we consider the continuous constant-Q transform $Y: \mathbb{R} \times \mathbb{R} \rightarrow \mathbb{C}$ of a signal $X \in L_\infty(\mathbb{R})$ with a window $w \in L_1(\mathbb{R})$, both of which are real-valued:

$$Y(f, t) = \mathcal{Q}_w X(f, t) := \frac{|f|}{f_{\min}} \int_{-\infty}^{\infty} X(s) w\left(\frac{f}{f_{\min}}(s - t)\right) e^{-i2\pi f s} ds,$$

where $f_{\min} > 0$ is a scaling factor.

The resulting spectrogram is shift-invariant: If we consider $X(t) = \cos(2\pi\nu t)$ with $\nu > 0$, then the resulting constant-Q transform is:

$$\begin{aligned}
Y(f, t) &= \frac{|f|}{f_{\min}} \int_{-\infty}^{\infty} \frac{e^{-i2\pi\nu s} + e^{i2\pi\nu s}}{2} w\left(\frac{f}{f_{\min}}(s-t)\right) e^{-i2\pi f s} ds \\
&= \frac{1}{2} \mathcal{F}w\left(f_{\min}\left(1 + \frac{\nu}{f}\right)\right) e^{-i2\pi(f+\nu)t} + \frac{1}{2} \mathcal{F}w\left(f_{\min}\left(1 - \frac{\nu}{f}\right)\right) e^{-i2\pi(f-\nu)t},
\end{aligned}$$

where $\mathcal{F}: L_1(\mathbb{R}) \rightarrow L_\infty(\mathbb{R})$ is the Fourier transform operator [cf. 24, 6, 15] with:

$$\mathcal{F}w(f) := \int_{-\infty}^{\infty} w(t) e^{-i2\pi f t} dt.$$

For $f > 0$, the first summand is zero if $\text{supp}(\mathcal{F}w) \subseteq [-f_{\min}, f_{\min}]$. The modulus of the second summand only depends on the ratio ν/f , making the magnitude of the spectrogram shift-invariant on a logarithmic frequency axis.

We would like to select w and therefore also $\mathcal{F}w$ as Gaussians with standard deviations ζ and $\sigma = 1/(2\pi\zeta)$, but then they will have unbounded support. This means that we must choose f_{\min} large enough such that $\mathcal{F}w$ has sufficiently decayed at this frequency. A logarithmic axis transform on the frequency axis $\alpha(f) = \alpha_0 \ln(f/f_0)$ with arbitrarily parameters $\alpha_0, f_0 > 0$ leads to an inverse $f(\alpha) = f_0 e^{\alpha/\alpha_0}$. For the magnitude of the dominant term in $Y(f, t)$, we then obtain:

$$\begin{aligned}
\mathcal{F}w\left(f_{\min}\left(1 - \frac{\nu}{f}\right)\right) &= \mathcal{F}w\left(f_{\min}\left(1 - \frac{\nu}{f_0 e^{\alpha/\alpha_0}}\right)\right) \\
&= \sqrt{2\pi}\zeta f_{\min} \exp\left(\frac{(2\pi\zeta f_{\min})^2}{2} \left(1 - \frac{\nu}{f_0 e^{\alpha/\alpha_0}}\right)^2\right),
\end{aligned}$$

which is not Gauss-shaped when regarded as a function of α , but we can approximate the mapping $\alpha \mapsto 1 - \frac{\nu}{f_0 e^{\alpha/\alpha_0}}$ by its linear approximation at $\alpha = \alpha_0 \ln(\nu/f_0)$:

$$1 - \frac{\nu}{f_0 e^{\alpha/\alpha_0}} = \frac{\alpha - \alpha_0 \ln(\nu/f_0)}{\alpha_0} + O((\alpha - \alpha_0 \ln(\nu/f_0))^2),$$

leading to a scaled Gaussian with mean $\mu = \alpha_0 \ln(\nu/f_0)$ and standard deviation $\sigma = \alpha_0/(2\pi\zeta f_{\min})$. Again, the validity of this approximation depends on the value of $\mathcal{F}w(f_{\min})$.

To check the second requirement, we need to regard the generalized Fourier transform on the space of tempered distributions:

$$Y(f, t) = \mathcal{Q}_w X(f, t) := \mathcal{F}\Xi_{f,t}(f), \quad \text{where} \quad \Xi_{f,t} = \frac{|f|}{f_{\min}} X \cdot w\left(\frac{f}{f_{\min}}(\cdot - t)\right),$$

with $X \in \mathcal{S}'(\mathbb{R})$, $w \in \mathcal{S}(\mathbb{R})$, and with $\mathcal{F}\Xi_{f,t} \in \mathcal{S}'(\mathbb{R})$ assumed to be representable as a complex-valued function (cf. [24] for the mathematical background).

For the response to a δ -transient at $t = t_0$, we then obtain:

$$Y(f, t) = \frac{|f|}{f_{\min}} w\left(\frac{f}{f_{\min}}(t_0 - t)\right) e^{-i2\pi f t_0},$$

whose modulus is not frequency-uniform. On the other hand, we know that if w is Gauss-shaped, we can convolve it with another Gaussian in order to attain the same variance for

all frequencies. We thus define:

$$U(\alpha, t) := \sqrt{\frac{f(\alpha)^2}{f(\alpha)^2 - f_{\min}^2}} \int_{-\infty}^{\infty} |\mathcal{Q}_w(f(\alpha), t - s)| w\left(\sqrt{\frac{f(\alpha)^2}{f(\alpha)^2 - f_{\min}^2}} s\right) ds.$$

with $w(s) = e^{-s^2/(2\zeta^2)}/\sqrt{2\pi\zeta^2}$. This is only valid for $f(\alpha) > f_{\min}$. For $f(\alpha) = f_{\min}$, we can just use $|\mathcal{Q}_w(f_{\min}, t)|$ without the convolution, but for $f(\alpha) < f_{\min}$, we would need to solve a deconvolution problem, which is ill-posed. This means that f_{\min} is actually the minimum frequency which can be resolved in the spectrogram.

It is natural to choose $f_0 = f_{\min}$. In this case, $\alpha(f_{\min}) = \alpha(f_0) = 0$, while α_0 can still be used to scale the frequency axis.

In practice, the convolution is carried out in the discrete domain, which introduces some error, but with sufficiently large resolution, this is rather low. It is, however, important to fix the ℓ_1 norm of the convolution kernel.

2.2 Wideband Signals

The problem with the previously discussed computation of the spectrogram comes from the Heisenberg inequality: Frequencies below f_{\min} cannot be resolved because the time-domain response would be too long, and setting f_{\min} too low deteriorates frequency resolution and introduces artifacts.

In general, any attempt to overcome this limitation would lead to an ill-posed problem. On the other hand, we know that the sound of many musical instruments can be represented as a sum of sinusoids, which correspond to Gaussian peaks in the frequency domain. With the short-time Fourier transform [cf. 15]

$$Z(f, t) = \mathcal{F}_w X(f, t) := \int_{-\infty}^{\infty} X(s) w(s - t) e^{-i2\pi fs} ds$$

and $X(t) = \cos(2\pi\nu t)$, we get:

$$Z(f, t) = \frac{1}{2} \mathcal{F}w(f + \nu) e^{-i2\pi(f+\nu)t} + \frac{1}{2} \mathcal{F}w(f - \nu) e^{-i2\pi(f-\nu)t}.$$

In Section 4.1, we introduce Algorithm 2 that can be used to identify patterns of peaks in a given logarithmic frequency spectrum. We can use the same algorithm to identify individual peaks in the linear frequency spectrum $Z(\cdot, t)$ (or rather its discretized version $Z[\cdot, k]$), apply the logarithm to their position, and thereby mimic the effect of the constant-Q transform while also preserving vertical alignment.¹ This “tricks” the Heisenberg inequality by using prior information about the shape of the peaks.

With this method, we can choose f_0 to be the lowest frequency that we aim to represent, while f_{\min} is merely a virtual quantity that indicates the frequency at which the same time-frequency resolution could still be achieved by the narrowband method.

¹For efficiency, we choose parameters $p = q = 1$. We assume a single instrument with $N_{\text{har}} = 1$ and set a sparsity condition of $N_{\text{ton}} = 1000$ with $\lambda = 1$. Rather than selecting one frequency with the highest cross-correlation at a time, we select the 1000 highest peaks with a dominance of more than 2 pixels.

3 Instrument Dictionary Representation of the Signal

3.1 Dictionary Layout and Parameters

Our dictionary is a two-dimensional data structure $D \in \mathbb{R}^{N_{\text{har}} \times N_{\text{ins}}}$, which is used to represent a discrete magnitude spectrogram $U[\alpha, k]$, $\alpha, k \in \mathbb{Z}$, with $U[\alpha, k] = U(\alpha, t)$, $k = \gamma t$, where $\gamma > 0$ is the time-sampling period for the spectrogram (with the scaling of the frequency axis determined by α_0). The number of tones is limited to N_{ton} . For each $k = 1, \dots, n$, we declare an index set $\mathcal{J}_k \subset \mathbb{N}$ for the parameters $a_{k,j}, \mu_{k,j}, \sigma_{k,j}, b_{k,j} \geq 0$ and $\eta_{k,j} \in \{1, \dots, N_{\text{ins}}\}$, $j \in \mathcal{J}_k$, where $a_{k,j}$ is the amplitude of a certain instrument tone, $\mu_{k,j}$ is the logarithmic fundamental frequency, $\sigma_{k,j}$ is the standard deviation of the corresponding Gaussian, $b_{k,j}$ is the inharmonicity, and $\eta_{k,j}$ is the selected instrument.

A simple model for many musical instruments is the wave equation, which has sinusoidal solutions at frequencies $f_h = hf_1^\circ$, $h = 1, \dots, N_{\text{har}}$, where $f_1^\circ > 0$ is the fundamental frequency. However, many string instruments (especially the piano with its high-tension strings) have non-negligible stiffness in their strings, leading to a fourth-order equation, which has solutions $f_h = (1 + bh^2)^{1/2}hf_1^\circ$, with the inharmonicity parameter $b > 0$ [cf. 12]. Applying the logarithm to both sides, this leads to $\ln(f_h) = \frac{1}{2} \ln(1 + bh^2) + \ln(hf_1^\circ)$.

Thus, a simple model for generating the spectrogram is:

$$u[\alpha, k] = \sum_{j \in \mathcal{J}_k} \sum_{h=1}^{N_{\text{har}}} a_{k,j} D[h, \eta_{k,j}] \exp\left(-\frac{(\alpha - \mu_{k,j} - \alpha_0 (\ln(h) + \frac{1}{2} \ln(1 + b_{k,j}h^2)))^2}{2\sigma_{k,j}^2}\right),$$

with $\alpha, k \in \mathbb{Z}$, and with $\alpha_0 > 0$ from Section 2.1. However, the magnitude spectrogram is not linear; in general, tones will interfere, creating beats. If the signals are uncorrelated (i.e., their inner product is 0), the squares will add linearly; to account for this, we define:

$$(u_p[\alpha, k])^p := \sum_{j \in \mathcal{J}_k} a_{k,j}^p (u_{p, \eta_{k,j}, j}[\alpha, k])^p$$

with

$$(u_{p, \eta, j}[\alpha, k])^p := \sum_{h=1}^{N_{\text{har}}} D[h, \eta]^p \exp\left(-\frac{(\alpha - \mu_{k,j} - \alpha_0 (\ln(h) + \frac{1}{2} \ln(1 + b_{k,j}h^2)))^2 p}{2\sigma_{k,j}^2}\right),$$

choosing $p = 2$.

3.2 Loss Term and Non-Linear Scaling

From one of the methods of either Section 2.1 or Section 2.2, we are given a measured magnitude spectrogram $U = (U[\alpha, k])_{\alpha, k \in \mathbb{Z}}$, which in practice has a finite size, such that $\text{supp}(U) \subseteq \{0, \dots, m-1\} \times \{0, \dots, n-1\}$, with $m, n \in \mathbb{N}$.

The straight-forward loss term is then given by the Frobenius norm as $R_{\mathcal{K}} = \frac{1}{2} \|U[\cdot, \mathcal{K}] - u_2[\cdot, \mathcal{K}]\|_{\text{F}}$, where \mathcal{K} is either an index set or a single index. However, it turns out that this is not a good distance measure for clustering tones from different instruments; this loss puts a large penalty on deviations in the lowest harmonics, but it is hardly influenced by the presence of higher harmonics.

The problem is that higher harmonics typically decay very quickly in power and are thus ignored by the Frobenius norm, while the human ear can still perceive them clearly. Our heuristic approach is to “lift” those harmonics using a concave power function:

$$R_{\mathcal{K},q} := \frac{1}{2} \left\| (U[\cdot, \mathcal{K}])^q - (u_2[\cdot, \mathcal{K}])^q \right\|_F^2, \quad 0 < q \leq 1.$$

The right choice of q is always a compromise: Choosing it too close to 1 will not have a sufficient effect, but choosing it too low makes the problem very non-convex, leading to computational issues. In practice, square root scaling with $q = 1/2$ produces good results.

4 Algorithmic Approach

In order to train the dictionary, we pursue a stochastic alternating-optimization approach. First the dictionary is initialized; for this, we generate a uniformly distributed random vector $d \in [0, 1]^{N_{\text{har}}}$ and an exponent $e \in [1, \infty)$ that is Pareto-distributed with a scale parameter of 2, and we set $D[h, \eta] = d[h]/h^e$. The initialization function and the main procedure are listed in Algorithm 1.

Algorithm 1: Dictionary initialization and main program

```

function init():
    e ← Par(1, 2)
    for h = 1, ..., Nhar:
        d[h] ← U[0, 1)
        d[h] ← d[h]/he
    return d[.]

for η = 1, ..., Nins:
    D[·, η] ← init()
loop a multiple of Nprn times:
    k ← random({0, ..., n - 1})
    Jk, ak, Jk, μk, Jk, σk, Jk, bk, Jk, ηk, Jk, A ← pursuit(D, U, k, A)
    D, τ, v1, v2 ← adam(D, τ, v1, v2, U, k, Jk, ak, Jk, μk, Jk, σk, Jk, bk, Jk, ηk, Jk)
    if min(τ) mod Nprn = 0:
        I ← renew(A)
for k = 0, ..., n - 1:
    Jk, ak, Jk, μk, Jk, σk, Jk, bk, Jk, ηk, Jk, A ← pursuit(D[·, I], U, k, A)

```

Given an initial dictionary, a random time frame $U[\cdot, k]$ of the measured spectrogram is chosen, and a sparse dictionary representation is computed. Afterwards, the dictionary is updated and the process is repeated.

4.1 Sparse Identification

The pursuit algorithm (Algorithm 2) is roughly based on orthonogonal matching pursuit (OMP) [27], but it also incorporates ideas from subspace pursuit [10]. For each $k =$

$0, \dots, n - 1$, the parameters are initialized as $a_{k,j}, b_{k,j}, \mu_{k,j} = 0$ and $\sigma_{k,j} = \alpha_0 / (2\pi\zeta f_{\min})$ for $j = 1, \dots, N_{\text{ton}} + 1$. The residual is initialized with $r_k = (U[\cdot, k])^q$.

In each step, an index $j \in \{1, \dots, N_{\text{ton}} + 1\}$ for which $a_{k,j} = 0$ is picked. The cross-correlation between the residual and the spectra of the individual instruments is computed as:

$$\rho_{k,j}[\alpha, \eta] = \sum_{i=0}^{m-1} \frac{r_k[i] (u_{2,\eta,j}[i - \alpha, k])^q}{\|(u_{2,\eta,j}[\cdot, k])^q\|_2}.$$

In order to accelerate this computation via the FFT [cf. 23], it is favorable to choose m as a power of 2.

Then, $\alpha \in \{0, \dots, m - 1\}$ and $\eta \in \{1, \dots, N_{\text{ins}}\}$ are chosen such that $\rho_{k,j}[\alpha, \eta]$ is maximized, and they are assigned to $\mu_{k,j}$ and $\eta_{k,j}$. The amplitude is picked as $a_{k,j}^q \leftarrow \rho_{k,j}[\mu_{k,j}, \eta_{k,j}] / \|(u_{2,\eta_{k,j,j}}[\cdot, k])^q\|_2$, provided that this value is greater than 0.

After this, for all the indices $j = 1, \dots, N_{\text{ton}} + 1$ for which $a_{k,j} > 0$ holds, the values $a_{k,j}, \mu_{k,j}, \sigma_{k,j}, b_{k,j}$ are refined via non-linear optimization in order to minimize R_q . For this purpose, we use the L-BFGS-B algorithm [9, 30, 22]. For all tones for which the amplitude hits the zero bound (i.e., $a_{k,j} = 0$), the parameters are reset to their initial value. Afterwards, the number of non-zero amplitudes is limited to N_{ton} by also resetting the parameters for the tones with the lowest amplitudes (which may affect at most one tone in this case). The non-linear optimization process is then run again.

In preparation for the next step, the residual is updated as $r_k \leftarrow (U[\cdot, k])^q - (u_2[\cdot, k])^q$. It is required that each step decreases the Euclidean norm of the residual by factor of $1 - \lambda$, $\lambda \in (0, 1]$; otherwise, the result of the current step is discarded, and the parameters from the previous step are returned.

The total number of iterations is limited to a value that is appropriate for the number of tones to identify.

4.2 Dictionary Update

Classically, dictionary learning is performed via factorization methods such as NMF [21, 20], K-SVD [2], or tensor factorization. These methods depend on a very specific structure of the problem, and they become slow when the amount of data is large.

While the use of stochastic gradient descent for such problems has been common for many years [cf., e.g., 1], new methods have been arising very recently due to their applications in deep learning. One of the most popular methods for this purpose is ADAM [19]. Its underlying idea is to treat the gradient as a random variable and, for each component, estimate its first moments as v_1 and its second moments as v_2 , and choose the step size proportional to $v_1 / \sqrt{v_2}$. If the derivative of the i th component is constant, then $v_1[i] / \sqrt{v_2[i]} = \pm 1$, in which case a large step size can be used. If the derivative oscillates a lot, however, then $v_1[i] / \sqrt{v_2[i]}$ will also be small and thereby dampen the oscillation in that direction.

The standard formulation of ADAM is completely independent of the scale of the derivatives. This makes it easy to control the absolute step size of the components, but it destroys the Landweber regularization property of regular gradient descent, which automatically decreases the step size for components whose partial derivative is small, taking into account the scaling of different harmonics.

Algorithm 2: Sparse identification algorithm

function pursuit(D, U, k, A):

$$r_k \leftarrow (U[\cdot, k])^q$$

$$\mathcal{J}_k \leftarrow \emptyset$$

loop N_{itr} times:

$$a_{k,j}, b_{k,j}, \mu_{k,j} \leftarrow 0, \sigma_{k,j} \leftarrow \alpha_0 / (2\pi\zeta f_{\min}) \text{ for } j \in \{1, \dots, N_{\text{ton}} + 1\} \setminus \mathcal{J}_k$$

$$j \leftarrow \min(\{1, \dots, N_{\text{ton}} + 1\} \setminus \mathcal{J}_k)$$

$$\rho_{k,j}[\alpha, \eta] \leftarrow \sum_{i=0}^{m-1} r_k[i] (u_{2,\eta,j}[i - \alpha, k])^q / \|(u_{2,\eta,j}[\cdot, k])^q\|_2$$

$$\mu_{k,j}, \eta_{k,j} \leftarrow \arg \max_{\alpha, \eta} \rho_{k,j}[\alpha, \eta]$$

$$a_{k,j}^q \leftarrow \rho_{k,j}[\mu_{k,j}, \eta_{k,j}] / \|(u_{2,\eta_{k,j,j}}[\cdot, k])^q\|_2$$

$$\mathcal{J}_k \leftarrow \mathcal{J}_k \cup \{j\}$$

$$a_{k,\mathcal{J}_k}, \mu_{k,\mathcal{J}_k}, \sigma_{k,\mathcal{J}_k}, b_{k,\mathcal{J}_k} \leftarrow \text{bfgs}(R_q), a_{k,\mathcal{J}_k} \geq 0$$

$$\mathcal{J}_k \leftarrow (\arg \text{sort}_{j \in \{1, \dots, N_{\text{ton}} + 1\}} a_{k,j} > 0)[1, \dots, N_{\text{ton}}]$$

$$a_{k,\mathcal{J}_k}, \mu_{k,\mathcal{J}_k}, \sigma_{k,\mathcal{J}_k}, b_{k,\mathcal{J}_k} \leftarrow \text{bfgs}(R_q), a_{k,\mathcal{J}_k} \geq 0$$

$$\theta_k \leftarrow \|r_k\|_2$$

$$r_k \leftarrow (U[\cdot, k])^q - (u_2[\cdot, k])^q$$

if $\|r_k\|_2 \geq (1 - \lambda)\theta$: **break**

$$A[\eta] \leftarrow A[\eta] + \sum_{\eta_{k,j}=\eta} a_{k,j}$$

return $\mathcal{J}_k, a_{k,\mathcal{J}_k}, \mu_{k,\mathcal{J}_k}, \sigma_{k,\mathcal{J}_k}, b_{k,\mathcal{J}_k}, \eta_{k,\mathcal{J}_k}, A$

Our first modification to ADAM is that while we still estimate the first moments for each dictionary entry (i.e., for each instrument and for each harmonic), we only compute one second moment estimate for each instrument, which is the arithmetic mean over the all the estimates for the harmonics.

Furthermore, we require all entries in the dictionary to be non-negative, since negative harmonic amplitudes would be unphysical. For consistency, we also require that no entries be larger than 1, so we end up with the box constraint that $D[h, \eta] \in [0, 1]$ for $h = 1, \dots, N_{\text{har}}$, $\eta = 1, \dots, N_{\text{ins}}$. To enforce this, we project each component to $[0, 1]$ after the end of a step.

Finally, we have to tackle the problem that dictionary entries for a particular instrument may diverge such they will not be used by the identification algorithm any more. For this purpose, we track the sum of the amplitudes associated with a specific instrument in the past. In regular intervals (every N_{prn} steps in Algorithm 1), we sort the instruments in the dictionary by their ratio of amplitude sum over the number of iterations for which they have existed (minus a small head start that benefits new instrument entries); then, we prune the dictionary by resetting the entries for those instruments where the ratio is lowest.

The dictionary learning algorithm and the renewal function are listed Algorithm 3. We use the default values of $\beta_1 = 0.9$, $\beta_2 = 0.999$, $\varepsilon = 10^{-8}$, and the step-size of $\kappa = 10^{-3}$. The head start is half the length of the pruning interval: $\tau_0 = N_{\text{prn}}/2$.

Algorithm 3: Dictionary learning algorithm (modified ADAM)

function `adam`($D, \tau, v_1, v_2, U, k, \mathcal{J}_k, a_{k, \mathcal{J}_k}, \mu_{k, \mathcal{J}_k}, \sigma_{k, \mathcal{J}_k}, b_{k, \mathcal{J}_k}, \eta_{k, \mathcal{J}_k}$) :

```

 $g \leftarrow \nabla_D R_{k,q}$ 
for  $\eta = 1, \dots, N_{\text{ins}}$  :
     $\tau[\eta] \leftarrow \tau[\eta] + 1$ 
     $v_1[\cdot, \eta] \leftarrow \beta_1 \cdot v_1[\cdot, \eta] + (1 - \beta_1) \cdot g[\cdot, \eta]$ 
     $v_2[\eta] \leftarrow \beta_2 \cdot v_2[\eta] + (1 - \beta_2) \cdot \text{mean}(g[\cdot, \eta]^2)$ 
     $\hat{v}_1[\cdot, \eta] \leftarrow v_1[\cdot, \eta] / (1 - \beta_1^{\tau[\eta]})$ 
     $\hat{v}_2[\eta] \leftarrow v_2[\eta] / (1 - \beta_2^{\tau[\eta]})$ 
     $D[\cdot, \eta] \leftarrow D[\cdot, \eta] - \kappa \cdot \hat{v}_1[\cdot, \eta] / (\sqrt{\hat{v}_2[\eta]} + \varepsilon)$ 
     $D[\cdot, \eta] \leftarrow \max(0, \min(1, D[\cdot, \eta]))$ 
return  $D, \tau, v_1, v_2$ 

```

function `renew`(A) :

```

 $\mathcal{I} \leftarrow (\text{arg sort}_{\eta \in \{1, \dots, N_{\text{ins}}\}} A[\eta] / (\tau[\eta] - \tau_0)) [1, \dots, N_{\text{ins}}/2]$ 
 $\tau[\mathcal{I}^c] = 0, v_1[\cdot, \mathcal{I}^c] = 0, v_2[\mathcal{I}^c] = 0, A[\mathcal{I}^c] = 0$ 
for  $\eta \in \mathcal{I}^c$  :
     $D[\cdot, \eta] \leftarrow \text{init}()$ 
return  $\mathcal{I}$ 

```

4.3 Resynthesis

After the dictionary has been trained by alternating between Algorithms 2 and 3, we represent the entire recording by running Algorithm 2 on each time frame $U[\cdot, k]$, $k = 0, \dots, n - 1$. This time, however, we need a linear-frequency spectrogram, and therefore apply the reverse transformation $f(\alpha) = f_0 e^{\alpha/\alpha_0}$ on the means of the Gaussians:

$$(z_{p,\eta}[f, k])^p := \sum_{\substack{j \in \mathcal{J}_k \\ \eta = \eta_{k,j}}} a_{k,j}^p (z_{p,\eta_{k,j}}[\alpha, k])^p, \quad (z_p[f, k])^p := \sum_{j \in \mathcal{J}_k} a_{k,j}^p (z_{p,\eta_{k,j}}[\alpha, k])^p,$$

with

$$(z_{p,\eta,j}[f, k])^p := \sum_{h=1}^{N_{\text{har}}} D[h, \eta]^p \exp\left(-\frac{(f - f(\mu_{k,j}) \cdot h(1 + b_{k,j}h^2)^{1/2})^2 p}{2(N_{\text{fft}} f_{\text{min}} \sigma_{k,j})^2 / (f_s \alpha_0)^2}\right).$$

For the reconstruction of the time-domain signal, we use the classical algorithm by Griffin and Lim [14] with an FFT length of N_{fft} and f_s is the sampling frequency. In order to have an identical standard deviation in the linear-frequency and log-frequency spectrograms, we choose $N_{\text{fft}} f_{\text{min}} = f_s \alpha_0$.

While more sophisticated methods have been developed recently, the original algorithm is very robust and simple. As an initial value, it accepts the original unseparated time-domain signal, namely:

$$Z[f, k] := Z(f \cdot f_s / N_{\text{fft}}, k / \gamma).$$

4.4 Spectral Masking

As an optional post-processing step on the spectrogram, we can mask the spectrograms from the dictionary representation with the spectrogram from the original recording. This method was proposed in [16, 17]; we choose to modify it by taking the element-wise square root of the mask proposed therein. With, again, $p = 2$, we then have:

$$\tilde{z}_{p,\eta}[f, k] := \frac{z_{p,\eta}[f, k]}{z_p[f, k]} \cdot Z[f, k].$$

In practice, a tiny value is added to the denominator in order to avoid division by zero.

With the procedure, we make sure that the synthesized spectrograms do not have any artifacts at frequencies that are not present in the original recording. Another benefit is mentioned in [16]: In cases where the sound of an instrument is not perfectly invariant w.r.t. pitch and volume, the masking can correct this. Furthermore, the phase of the complex-valued Z provides a good approximation for the phase of the separated spectrogram.

5 Experimental Evaluation

We choose a sampling frequency of $f_s = 48000$ Hz and an FFT length of $N_{\text{fft}} = 12 \cdot 1024 = 12288$. With $\zeta = 1024/f_s$, this means that we cut the windowed signal at $\pm 6\zeta$.

We aim to represent frequencies from 20 Hz up to (and not including) 20480 Hz; the log-frequency spectrogram should be $m = 1024$ pixels high. Thus, we set $f_0 = 20$ Hz and $\alpha_0 = 1024 / \ln(20480 \text{ Hz} / 20 \text{ Hz}) = 1024 / \ln(1024)$. Furthermore, we choose $\gamma = 256/f_s$. Due

to $f_{\min} = f_s \alpha_0 / N_{\text{fft}} = 4000 / \ln(1024) > f_0$, the method from Section 2.1 is out of question, and we must use the method from Section 2.2.

For the dictionary, we use $N_{\text{har}} = 25$ harmonics and a pruning interval of $N_{\text{prn}} = 500$ in the training.

The code is written for Python 3.5 and was tested with NumPy 1.12.1, SciPy 0.18.1, PyFFTW 0.10.4, and Matplotlib 2.1.0. The narrowband method requires Tensorflow of at least version 0.13.

5.1 Performance Measures

Vincent et al. [28] define the signal-to-distortion ratio (SDR), the signal-to-interference ratio (SIR), the signal-to-noise ratio (SNR), and the signal-to-artifacts ratio (SAR). Assuming original signals $(X_\eta)_{\eta=1, \dots, N_{\text{ins}}}$, additive noise signals $(\Gamma_\eta)_{\eta=1, \dots, N_{\text{ins}}}$, and reconstructed signals $(x_\eta)_{\eta=1, \dots, N_{\text{ins}}}$, those quantities (to be interpreted in dB) are defined as:

$$\begin{aligned} \text{SDR}_\eta &= 10 \cdot \log_{10} \frac{\|\mathcal{P}_{X_\eta}(x_\eta)\|_2^2}{\|\mathcal{P}_{X_\eta}(x_\eta) - x_\eta\|_2^2}, & \text{SIR}_\eta &= 10 \cdot \log_{10} \frac{\|\mathcal{P}_{X_\eta}(x_\eta)\|_2^2}{\|\mathcal{P}_{X_\eta}(x_\eta) - \mathcal{P}_X(x_\eta)\|_2^2}, \\ \text{SNR}_\eta &= 10 \cdot \log_{10} \frac{\|\mathcal{P}_X(x_\eta)\|_2^2}{\|\mathcal{P}_X(x_\eta) - \mathcal{P}_{X,\Gamma}(x_\eta)\|_2^2}, & \text{SAR}_\eta &= 10 \cdot \log_{10} \frac{\|\mathcal{P}_{X,\Gamma}(x_\eta)\|_2^2}{\|\mathcal{P}_{X,\Gamma}(x_\eta) - x_\eta\|_2^2}, \end{aligned}$$

where \mathcal{P}_{X_η} is the orthogonal projection on X_η , while \mathcal{P}_X is the orthogonal projection on $(X_\eta)_{\eta=1, \dots, N_{\text{ins}}}$, and $\mathcal{P}_{X,\Gamma}$ is the orthogonal projection on $(X_\eta)_{\eta=1, \dots, N_{\text{ins}}}$ and $(\Gamma_\eta)_{\eta=1, \dots, N_{\text{ins}}}$. If the noise vectors are not known (which they are not, unless all noise was artificially added on an otherwise completely clean signal), they are assumed to be zero, and the noise will be treated as artifacts.

Originally, those measures are defined in the time-domain. This, however, makes them very sensitive to phase mismatch: The projection of a sinusoid on its 90°-shifted copy will be zero, even though the signals are otherwise identical.

We re-implemented the original MATLAB code in NumPy, adopting the convention to use the permutation of identified instruments with the highest summed SIR.

5.2 Artificial Data

To study the efficacy of the algorithm on perfectly consistent data without any artifacts or noise, we generate $N_{\text{ins}} = 2$ random instrument patterns via `init` in Algorithm 1. With this dictionary, we generate 10000 random time frames with $N_{\text{ton}} = 2$ tones at uniformly random fundamental log-frequencies $\alpha \in [0, 500)$, on which we train another dictionary. We then generate a log-frequency spectrogram with 10000 additional random time frames that we represent once with the original dictionary and once with the trained dictionary. We flatten the generated spectrogram and the spectrograms that we synthesized from the identified dictionary representations into vectors and apply the above performance measures.² The result from 5 runs is displayed in Table 1. No spectral masking was applied.

²Converting the spectrograms to the time-domain would not make sense, as they are almost surely inconsistent.

Table 1: Performance measures for the representation of artificial data, once with the original dictionary from which the data once generated and once with a dictionary that was trained on the data. The experiment was run 5 times with independent random data. The upper row corresponds to the first instrument, and the lower row corresponds to the second instrument, respectively. Higher is always better.

SDR (orig.)	SDR (trained)	SIR (orig.)	SIR (trained)	SAR (orig.)	SAR (trained)
36.8	31.1	72.1	67.2	36.8	31.1
35.0	34.0	70.3	72.7	35.0	34.0
40.1	33.1	92.5	64.5	40.1	33.1
34.0	39.9	67.1	102.1	34.0	39.9
37.3	35.1	71.3	69.4	37.3	35.2
35.1	34.1	69.7	70.1	35.1	34.1
37.8	35.6	87.6	90.0	37.8	35.6
34.3	33.2	65.8	70.6	34.3	33.2
16.8	15.2	32.9	67.2	16.9	15.2
15.3	16.8	71.5	32.9	15.3	16.9

It is apparent that the algorithm is capable of achieving good separation, while some instrument spectra pose greater difficulty than others. The difference from the representation with the original dictionary to the representation with trained dictionary is not substantial, and sometimes the latter is even better, so we conclude that the dictionary learning algorithm fulfills its purpose, leaving the pursuit algorithm as the bottleneck.

5.3 Real Data

We used the 8th piece from the 12 Bassett Horn Duos by Wolfgang A. Mozart (KV 487) in an arrangement by Alberto Gomez Gomez for two recorders³. The upper part was played on a soprano recorder, and the lower part was played on a violin. These instruments are easily distinguishable, as the recorder has an almost sinusoidal sound, while the sound of the violin is sawtooth-like, with strong harmonics [12].

The instrument tracks were recorded separately, while a metronome/“play-along” track was provided via headphones. Evenness of the tone was favored over musical expression. We combined the tracks by adding the two digital signals with no post-processing other than adjustment of overall timing and volume and let the algorithm run with 100000 training steps, with $N_{\text{ins}} = 2$ and $N_{\text{ton}} = 2$.

The quantitative results are displayed in Table 2. As can be expected, the recorder is universally better represented than the violin, and spectral masking leads to considerable improvements in both domains especially for the violin. This complies with the explanation in [16] that it helps represent instruments with more diverse spectra, as the violin has 4 different strings and its sound is very sensitive to technique.

³ [https://imslp.org/wiki/12_Horn_Duos,_K.487/496a_\(Mozart,_Wolfgang_Amadeus\)](https://imslp.org/wiki/12_Horn_Duos,_K.487/496a_(Mozart,_Wolfgang_Amadeus))

Table 2: Performance measures for the evaluation of the real data for each instrument, once in the time-domain and once in the linear-frequency spectral domain. The trained dictionary is always the same, and higher is always better.

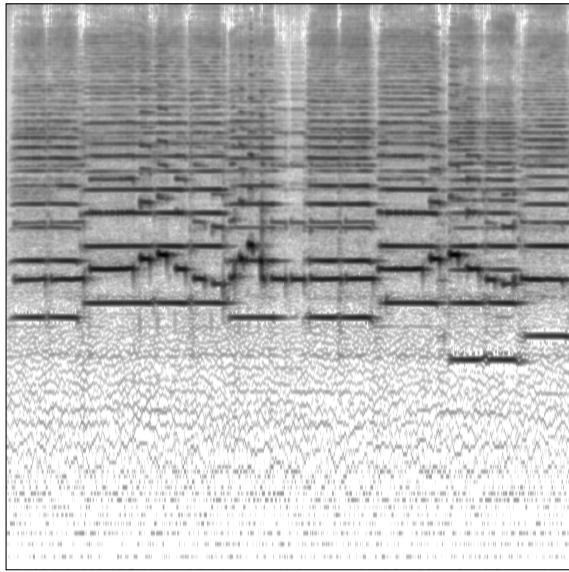
Masking	Domain	Instrument	SDR	SIR	SAR
Yes	Time	Recorder	14.5	31.8	14.5
		Violin	11.0	22.3	11.4
	Spectral	Recorder	13.9	46.9	13.9
		Violin	13.1	32.4	13.1
No	Time	Recorder	12.1	31.5	12.2
		Violin	6.8	23.1	6.9
	Spectral	Recorder	10.5	58.0	10.5
		Violin	7.1	34.3	7.1

For phase reconstruction, we used merely one iteration of the Griffin-Lim algorithm in order to preserve the phase of the original spectrogram as much as possible.

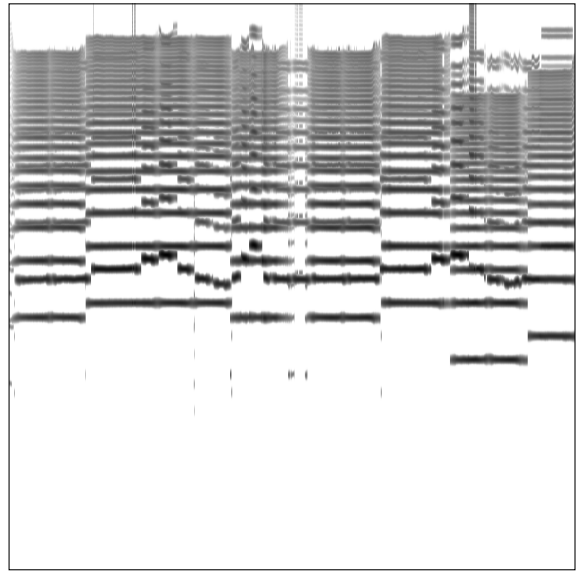
From qualitative assessment of the generated tracks, we state that while some artifacts and interference are audible, they provide a good aural impression of the actually played tracks. The only tone⁴ that is actually misidentified is a recorder tone that interferes with the even-numbered harmonics of the violin tone that is played at the same time and is one octave lower. In this case, the third harmonic of the violin tone is erroneously identified as the recorder tone.

Spectrograms of the original recording and the synthesized representations are displayed in Figure 1. The original spectrogram contains broad-spectrum components (“noise”) that do not fit the dictionary model and thus cannot be represented, so they are not found in the synthesized spectrograms. The choice of $N_{\text{har}} = 25$ must be regarded as a compromise: Although the sound of the violin could be represented more accurately with an even higher numbers of harmonics, this would increase both the computation time of the algorithm and also number of variables to be trained. The incorrectly identified recorder tone can be seen as the last tone in Figure 1c. It is not audible when the synthesized audio files are mixed back together.

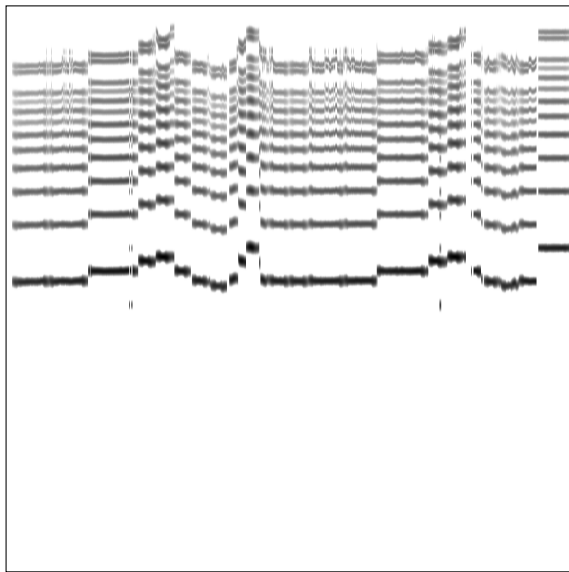
⁴which occurs 4 times in total, due to repetitions of the passage



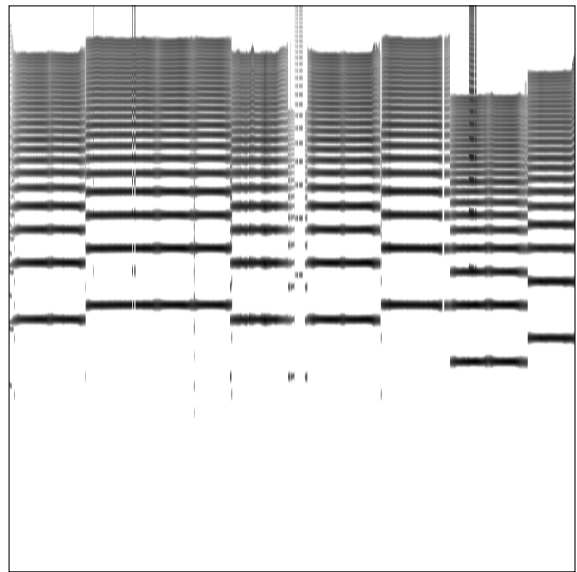
(a) Original, generated via the wideband method



(b) Synthesized, combined



(c) Synthesized recorder track



(d) Synthesized violin track

Figure 1: Log-frequency spectrograms for the recorded piece. Time on the horizontal axis goes from 0s to 8.4s, frequency on the vertical axis goes from 20 Hz to 20480 Hz. The grayscale axis is logarithmic and normalized to a dynamic range of 100 dB for each plot.

6 Conclusion and Future Work

The main improvements of our algorithm over previous ones are its ability to represent both narrowband and wideband audio signals properly and its flexibility to deal with instruments without making assumptions about their tuning. This makes it especially suitable for instruments where the exact frequency of a tone is not fixed by the construction of the instrument but at least partly depends on playing technique. The number of tones is instead limited by a sparsity condition.

We note, however, that blind source separation always requires favorable data, so it is not a “silver bullet” but rather a tool that is useful in specific situations when structural assumptions about the data can be made.

While a lot of research is currently going into deep learning rather than classical signal processing, it turns out that methods like the scattering transform [3] and ADAM [19] that were developed with deep learning in mind can be applied to both approaches.

The bottleneck of the presented method appears to be the pursuit algorithm, which is based on OMP. It may lead to an improvement if an ℓ_1 -based algorithm was used instead, like convolutional sparse coding [7]. The naive application of this method is hindered by the non-linear optimization step, however.

Acknowledgements

The authors would like to thank Bernhard G. Bodmann, Gitta Kutyniok, and Monika Dörfler for engaging discussions on the subject.

References

- [1] Michal Aharon and Michael Elad. “Sparse and redundant modeling of image content using an image-signature-dictionary”. In: *SIAM J. Imaging Sci.* 1.3 (2008), pp. 228–247.
- [2] Michal Aharon, Michael Elad, and Alfred Bruckstein. “K-SVD: An algorithm for designing overcomplete dictionaries for sparse representation”. In: *IEEE Trans. Signal Process.* 54.11 (2006), pp. 4311–4322.
- [3] Joakim Andén and Stéphane Mallat. “Deep scattering spectrum”. In: *IEEE Trans. Signal Process.* 62.16 (2014), pp. 4114–4128.
- [4] Peter Balazs, Monika Dörfler, Florent Jaillet, Nicki Holighaus, and Gino A. Velasco. “Theory, implementation and applications of nonstationary Gabor frames”. In: *J. Comput. Appl. Math.* 236.6 (2011), pp. 1481–1496.
- [5] William H. Barnes. *The Contemporary American Organ*. 8th ed. J. Fischer and Bro., 1964.
- [6] John J. Benedetto. *Harmonic Analysis and Applications*. CRC Press, 1996.
- [7] Hilton Bristow, Anders Eriksson, and Simon Lucey. “Fast convolutional sparse coding”. In: *Computer Vision and Pattern Recognition (CVPR), 2013 IEEE Conference on*. IEEE. 2013, pp. 391–398.

- [8] Judith C. Brown. “Calculation of a constant Q spectral transform”. In: *J. Acoust. Soc. Am.* 89.1 (1991), pp. 425–434.
- [9] Richard H. Byrd, Peihuang Lu, Jorge Nocedal, and Ciyou Zhu. “A limited memory algorithm for bound constrained optimization”. In: *SIAM J. Sci. Comput.* 16.5 (1995), pp. 1190–1208.
- [10] Wei Dai and Olgica Milenkovic. “Subspace pursuit for compressive sensing signal reconstruction”. In: *IEEE Trans. Inf. Theory* 55.5 (2009), pp. 2230–2249.
- [11] Derry Fitzgerald, Matt Cranitch, and Eugene Coyle. “Shifted non-negative matrix factorisation for sound source separation”. In: *Statistical Signal Processing, 2005 IEEE/SP 13th Workshop on.* IEEE, 2005, pp. 1132–1137.
- [12] Neville H. Fletcher and Thomas D. Rossing. *The Physics of Musical Instruments.* Springer Science & Business Media, 2012.
- [13] Gerald B. Folland and Alladi Sitaram. “The Uncertainty Principle: A Mathematical Survey”. In: *J. Fourier Anal. Appl.* 3.3 (1997), pp. 207–238.
- [14] Daniel Griffin and Jae Lim. “Signal estimation from modified short-time Fourier transform”. In: *IEEE Trans. Acoust., Speech, Signal Process.* 32.2 (1984), pp. 236–243.
- [15] Karlheinz Gröchenig. *Foundations of Time-Frequency Analysis.* Springer, 2001.
- [16] Rajesh Jaiswal, Derry FitzGerald, Dan Barry, Eugene Coyle, and Scott Rickard. “Clustering NMF basis functions using shifted NMF for monaural sound source separation”. In: *Acoustics, Speech and Signal Processing (ICASSP), 2011 IEEE International Conference on.* IEEE, 2011, pp. 245–248.
- [17] Rajesh Jaiswal, Derry Fitzgerald, Eugene Coyle, and Scott Rickard. “Shifted NMF using an efficient constant-Q transform for monaural sound source separation”. In: *22nd IET Irish Sig. and Sys. Conf.* IET, 2011.
- [18] Rajesh Jaiswal, Derry Fitzgerald, Eugene Coyle, and Scott Rickard. “Towards shifted NMF for improved monaural separation”. In: *24th IET Irish Signals and Systems Conference.* IET, 2013.
- [19] Diederik P. Kingma and Jimmy Ba. “Adam: A method for stochastic optimization”. In: *arXiv preprint arXiv:1412.6980* (2014).
- [20] Daniel D. Lee and H. Sebastian Seung. “Algorithms for non-negative matrix factorization”. In: *Adv. Neural Inf. Process. Syst.* 2001, pp. 556–562.
- [21] Daniel D. Lee and H. Sebastian Seung. “Learning the parts of objects by non-negative matrix factorization”. In: *Nature* 401.6755 (1999), pp. 788–791.
- [22] José Luis Morales and Jorge Nocedal. “Remark on “Algorithm 778: L-BFGS-B: Fortran subroutines for large-scale bound constrained optimization””. In: *ACM Trans. Math. Softw.* 38.1 (2011), p. 7.
- [23] Henri J. Nussbaumer. *Fast Fourier Transform and Convolution Algorithms.* Springer, 1981.
- [24] Walter Rudin. *Functional Analysis.* 2nd ed. McGraw-Hill, 1991.

- [25] Mikkel N. Schmidt and Rasmus K. Olsson. “Single-channel speech separation using sparse non-negative matrix factorization”. In: *Ninth International Conference on Spoken Language Processing*. 2006.
- [26] Paris Smaragdis and Judith C. Brown. “Non-negative matrix factorization for polyphonic music transcription”. In: *Applications of Signal Processing to Audio and Acoustics, 2003 IEEE Workshop on*. IEEE. 2003, pp. 177–180.
- [27] Joel A. Tropp and Anna C. Gilbert. “Signal recovery from random measurements via orthogonal matching pursuit”. In: *IEEE Trans. Inf. Theory* 53.12 (2007), pp. 4655–4666.
- [28] Emmanuel Vincent, Rémi Gribonval, and Cédric Févotte. “Performance measurement in blind audio source separation”. In: *IEEE Trans. Audio, Speech, Language Process.* 14.4 (2006), pp. 1462–1469.
- [29] Beiming Wang and Mark D. Plumbley. “Musical audio stream separation by non-negative matrix factorization”. In: *Proc. UK Digital Music Research Network (DMRN) Summer Conf.* 2005.
- [30] Ciyou Zhu, Richard H. Byrd, Peihuang Lu, and Jorge Nocedal. “Algorithm 778: L-BFGS-B: Fortran subroutines for large-scale bound-constrained optimization”. In: *ACM Trans. Math. Softw.* 23.4 (1997), pp. 550–560.